AIAA JOURNAL
Vol. 34, No. 11, November 1996

# Structural Damage Detection Using Real-Time Modal Parameter Identification Algorithm

Tae W. Lim*
*University of Kansas, Lawrence, Kansas 66045*
Albert Bosse†
*Swales and Associates, Inc., Beltsville, Maryland 20705*
and
Shalom Fisher‡
*U.S. Naval Research Laboratory, Washington, D.C. 20375-5355*

**A new approach to conducting structural damage detection is described. The approach employs a real-time modal parameter identification algorithm implemented in a digital-signal-processor-based data acquisition system. Because the modal parameter extraction process is conducted in real time, the algorithm is capable of identifying changes in structural properties attributable to structural damage as soon as they occur. Using the algorithm and a laboratory truss structure, it is demonstrated experimentally that continuous, real-time monitoring of anomalies attributable to structural damage is feasible. This monitoring capability will provide an early warning to an operator so that proper measures can be taken before a catastrophic failure occurs. The results of the damage detection study using the truss are presented along with the description of the real-time modal parameter identification algorithm.**

## Introduction

STRUCTURAL damage detection using modal test data has been investigated extensively over the past decade by many researchers[1] and for a wide range of problems, ranging from bridges[2] to offshore drilling platforms[3] to lightweight flexible structures.[4–10] Most of the algorithms demand a significant amount of modal test data and an accurate analytical model of the structure. These requirements make the damage detection procedures not only expensive and time-consuming but also impractical for real-life structures in service. Although successful damage detection investigations have been reported, they are mainly limited to laboratory truss structures,[4–7] and the emergence of a practical, mature technology appears to be a distant reality. Efforts also have been made to employ techniques such as artificial neural networks[8,9] in an attempt to minimize test data requirements, to reduce the burden of conducting modal parameter identification, and to diminish the role of a refined analytical model in the damage detection process.

The Naval Center for Space Technology at the U.S. Naval Research Laboratory (NRL) has been examining technologies for conducting health monitoring of spacecraft in orbit.[10] For envisioned large, flexible spacecraft to perform missions such as space-based interferometry, active control for vibration suppression is expected to play a significant role in meeting the performance objectives. Structural health monitoring of these actively controlled structures is important in maintaining not only structural integrity but also performance of controllers. Currently available damage detection methods, as described above, assume that accurate modal test data would be available periodically during the lifetime of the structure. For operating spacecraft, however, it will be prohibitively expensive to obtain the quantity and quality of modal test data required by the damage detection methods. This fundamental limitation undermines the possibility of successful implementation of these methods for spacecraft structural health monitoring.

Structural health monitoring typically includes detection, location, and quantification of structural damage. The focus of this paper is on structural damage detection using a real-time modal parameter identification algorithm,[11,12] although the algorithm is applicable to structural health monitoring. The adaptive algorithm processes a set of input and output time histories to extract modal parameters. Because the modal parameter extraction is conducted in real time, changes in structural dynamic properties can be monitored as the changes occur. This capability would allow the real-time detection of anomalies in the structure and provide an immediate alert for an appropriate action to be taken. This approach also has a potential of significantly reducing the instrumentation and data processing requirements of the current modal-test-data-based damage detection algorithms and the degree of dependency on the refined analytical model of the structure to conduct damage detection. The real-time modal parameter identification algorithm and its performance in detecting structural damage in a 12-bay laboratory space truss, referred to as the NRL space truss, is presented.

## Real-Time Modal Parameter Identification Algorithm

The basic concept and theoretical development of the real-time modal parameter identification algorithm are described briefly herein. Detailed information on the algorithm can be obtained elsewhere.[11,12]

### Design and Identification for Adaptive Filters

The basic building block of the algorithm is an adaptive filter that represents a single input/single output (SISO) system with structural modes to model the I/O behavior. To design the filter, consider the transfer function of a SISO system in the $s$ domain as

$$\frac{Y_q(s)}{U_p(s)} = \sum_{i=1}^{N} \frac{\phi_{p_i}\phi_{q_i}}{s^2 + 2\zeta_i\omega_i s + \omega_i^2} \tag{1}$$

where $Y_q(s)$ and $U_p(s)$ represent displacement at degree-of-freedom (DOF) $q$ and force input at DOF $p$, respectively; and $N$ is the number of modes used to represent the structural response; $\omega_i$ and $\zeta_i$ are the $i$th natural frequency in radians per second and the damping ratio, respectively; and $\phi_{p_i}$ and $\phi_{q_i}$ are the $i$th mode-shape coefficients at DOF $p$ and DOF $q$, respectively. The structural response is represented as a superposition of responses from the individual modes. Consider the $i$th mode only. Then, the transfer function in Eq. (1) is converted into the $z$ domain, using the bilinear transformation[13] of

$$s = 2f_s(z-1)/(z+1) \tag{2}$$

Received Feb. 22, 1996; revision received June 13, 1996; accepted for publication June 25, 1996; also published in *AIAA Journal on Disc*, Volume 2, Number 1. Copyright © 1996 by the American Institute of Aeronautics and Astronautics, Inc. All rights reserved.

*Assistant Professor, Department of Aerospace Engineering. Member AIAA.

†Senior Engineer, 5050 Powder Mill Road. Member AIAA.

‡Naval Center for Space Technology, Code 8220.

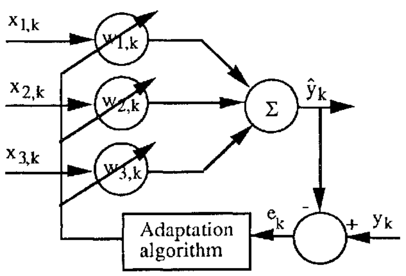


**Fig. 1 Block diagram of an adaptive filter.**

where $f_s$ is the sampling frequency in hertz. The resulting transfer function becomes

$$\frac{Y_q(z)}{U_p(z)} = \frac{(b_k/4f_s^2)(1 + 2z^{-1} + z^{-2})}{1 + a_{1k}z^{-1} + a_{2k}z^{-2}} \tag{3}$$

where the subscript $k$ indicates the values at time-step $k$ and the coefficients $b_k$, $a_{1k}$, and $a_{2k}$ are written as

$$b_k = \frac{\phi_{p_i}\phi_{q_i}}{1 + (\zeta_i\omega_i/f_s) + (\omega_i/2f_s)^2} \tag{4}$$

$$a_{1k} = \frac{-2 + (\omega_i^2/2f_s^2)}{1 + (\zeta_i\omega_i/f_s) + (\omega_i/2f_s)^2} \tag{5}$$

$$a_{2k} = \frac{1 - (\zeta_i\omega_i/f_s) + (\omega_i/2f_s)^2}{1 + (\zeta_i\omega_i/f_s) + (\omega_i + 2f_s)^2} \tag{6}$$

The transfer function in Eq. (3) is referred to as an infinite impulse response filter in the signal processing literature.[14]

Here, we define

$$x_{1,k} = u_k + 2u_{k-1} + u_{k-2} \qquad x_{2,k} = y_{k-1} \qquad x_{3,k} = y_{k-2} \tag{7}$$

and

$$w_{1,k} = b_k/4f_s^2 \qquad w_{2,k} = -a_{1k} \qquad w_{3,k} = -a_{2k} \tag{8}$$

where $u_k$ and $y_k$ correspond to $U_p(z)$ and $Y_q(z)$, respectively, at time-step $k$. Then, using the definitions given in Eqs. (7) and (8), the transfer function in Eq. (3) can be cast into the form of an adaptive filter shown in Fig. 1. If the filter coefficients in Eq. (8) are identified from the adaptive filter, then the transfer function in Eq. (3) will be identified readily. The filter coefficients of the adaptive filter in Fig. 1 are updated using the adaptive least-mean-square algorithm[14,15] as

$$w_{j,k+1} = w_{j,k} + 2\alpha_j e_k x_{j,k}, \qquad \text{for} \qquad j = 1, 2, 3 \tag{9}$$

where the positive constant $\alpha_j$ is the learning rate corresponding to the $j$th coefficient and determines the update rates for the coefficients. More information on the filter-coefficient update procedure is available elsewhere.[11,12]

### Modal Parameter Identification

The transfer function identified in the $z$ domain can be utilized to extract modal parameters. For instance, the transfer function in Eq. (3) can be transformed back into the $s$ domain using the inverse bilinear transformation of

$$z = \frac{2f_s + s}{2f_s - s} \tag{10}$$

The transformed transfer function then is written as

$$\frac{Y_q(s)}{U_p(s)} = \frac{[4b_k/(1 - a_{1k} + a_{2k})]}{s^2 + [4f_s(1 - a_{2k})/(1 - a_{1k} + a_{2k})]s + [4f_s^2(1 + a_{1k} + a_{2k})/(1 - a_{1k} + a_{2k})]} \tag{11}$$

By examining the transfer function in Eq. (11) in comparison to the transfer function in Eq. (1), it can be seen easily that natural frequency $\omega_i$ (rad/s), damping ratio $\zeta_i$, and mode-shape amplitude $\phi_{p_i}\phi_{q_i}$ for the $i$th mode are related to the adaptive-filter coefficients as follows:

$$\omega_i = 2f_s\sqrt{\frac{1 + a_{1k} + a_{2k}}{1 - a_{1k} + a_{2k}}} \tag{12}$$

$$\zeta_i = \frac{2f_s(1 - a_{2k})}{\omega_i(1 - a_{1k} + a_{2k})} \tag{13}$$

$$\phi_{p_i}\phi_{q_i} = \frac{4b_k}{1 - a_{1k} + a_{2k}} \tag{14}$$

where $f_s$ is the sampling frequency in hertz. The modal parameters in Eqs. (12–14) can be identified in real time as the transfer-function coefficients ($b_k$, $a_{1k}$, and $a_{2k}$) are updated in real time by the adaptive filter.

The algorithm described is capable of identifying modal parameters of one mode at a time. However, transducer signals obtained in actual tests typically have contributions from multiple modes. Thus, the algorithm cannot be applied directly in this situation and it needs the capability of identifying multiple modes simultaneously, which is not yet developed. To apply the algorithm herein, bandpass filters are used to extract a single frequency of interest from the signal. The algorithm then is applied to identify the corresponding modal parameters using the filtered signal. This filtering process may alter the amplitude of the frequency response function, depending on the separation of adjacent frequencies and the filter design. This alteration, however, will not be detrimental for structural damage detection purposes because the changes in the relative amplitude will be of primary concern and the changes in natural frequencies and damping ratios also will be used to conduct structural damage detection.

## Real-Time Structural Damage Detection of the NRL Truss

The real-time system identification algorithm described previously was employed for the structural damage detection of the NRL space truss. This section details the experiments and the findings.

### Description of the Experimental Apparatus

The NRL space truss shown in Figs. 2 and 3 represents a flexible spacecraft structure that may support solar arrays, scientific instrumentation, or sensor platforms. The truss is an assembly of batten/longeron and diagonal struts interconnected by node balls. The terminating ends of each strut are comprised of an outer sleeve, a screw, a nut, and a standoff. The outer sleeve and the tube are bonded using epoxy, and a tapered pin is inserted to prevent them from slipping. The standoff is attached to a node ball by the screw. The outer sleeve and the standoff are then joined by tightening the nut. The terminating end design allows easy removal of each strut without disturbing adjacent struts by unscrewing the nuts. Each strut consists of an aluminum tube of 0.79 cm o.d. with 0.89-mm wall thickness. The struts are 26.5 cm long for longerons/battens and 40.6 cm long for diagonals. The T-shaped truss is clamped at its base and is extended two bays vertically and 11 bays horizontally. Each bay is a cube with the side dimension of 34 cm.

A piezoceramic active strut is substituted for a diagonal truss member in the center bay of the truss, as shown in Fig. 3. The active strut provides an excitation source to the structure and is located where the second mode of the truss can be excited easily. The second mode exhibits a see-saw motion of the transverse boom in the vertical plane. For the second mode, the struts in the two vertical bays near the base of the truss experience the most of deformation, whereas the remaining horizontal bays move without significant deformation of individual struts. The active strut is mated

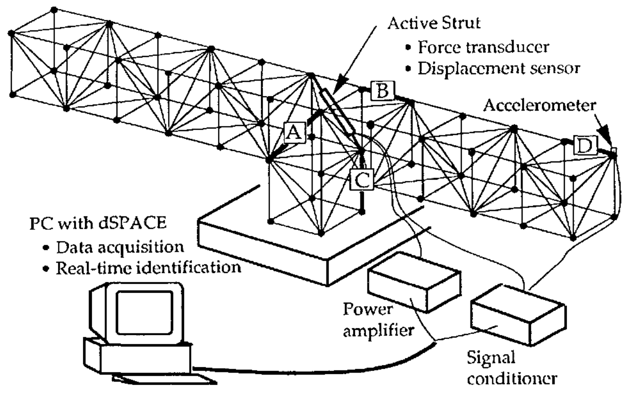


**Fig. 2 NRL space truss with test apparatus and damage locations.**

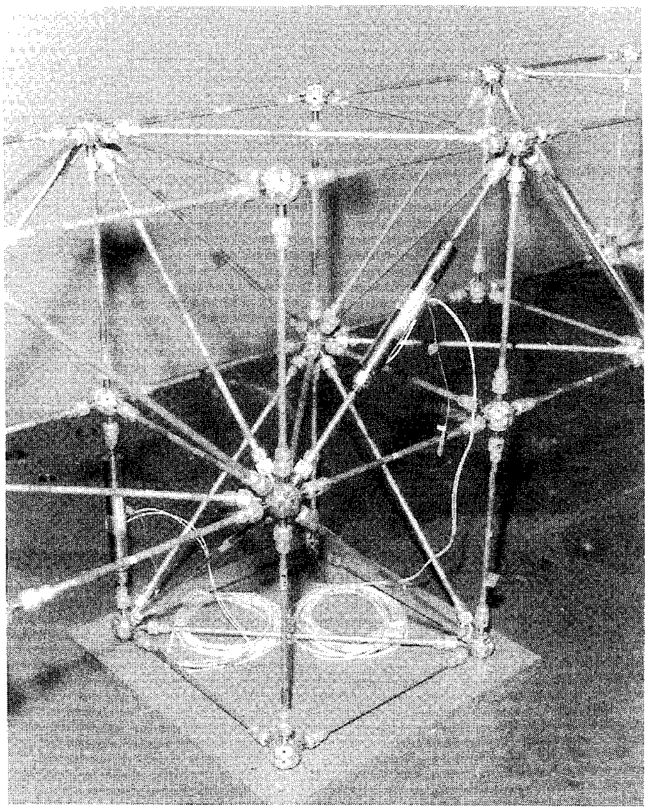

**Fig. 3 Active strut installed in the NRL truss (picture taken from the back of the truss).**

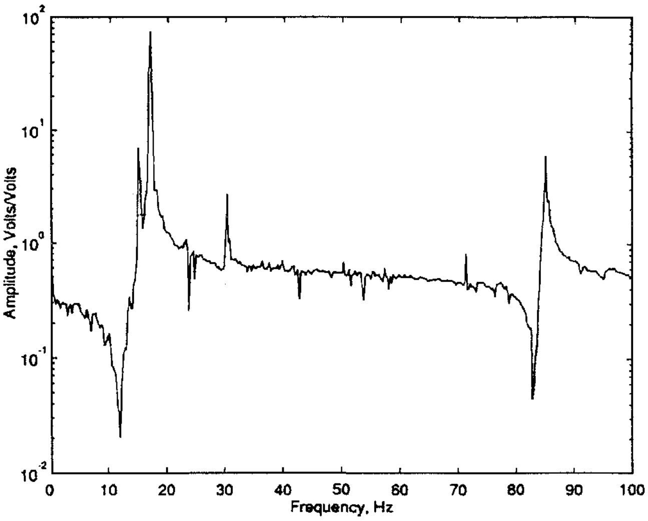


**a) Using force transducer signal**

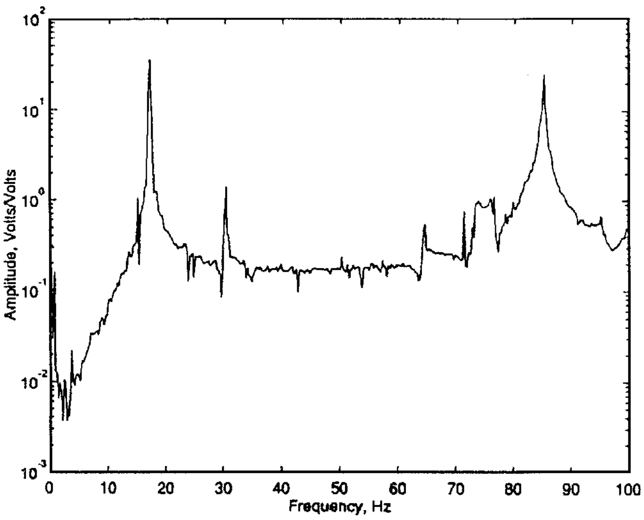


**b) Using accelerometer signal**

**Fig. 4 FRF at sensor locations.**

with a force transducer that is used to measure the axial force in the strut. The active strut used in this study was designed and fabricated at the Jet Propulsion Laboratory and is on loan to the NRL. Its construction and characteristics are similar to those described by Fanson et al.[16] The active strut consists of a preloaded stack of piezoceramic disks in a cylindrical housing with an embedded displacement sensor.

Data acquisition and real-time modal parameter identification were conducted using a high-speed digital-signal-processor (DSP) system. The DSP system consists of a TMS320C40 DSP chip and software interfaces including real-time interface (RTI), TRACE, and COCKPIT. A C-code is written for the implementation of the identification algorithm in the DSP system. RTI serves as an interface between the C-code written by a user and the DSP system by facilitating the process of downloading and running the C-coded algorithm. TRACE is used for real-time display of time histories and data recording, and COCKPIT is used to make real-time changes of the identification algorithm parameters while the DSP is running.

### System Identification Experiment

To conduct real-time identification experiments for damaged and undamaged structures, band-limited Gaussian noise (0–50 Hz) was generated by a signal generator. The signal then was used to drive the active strut located in the truss. The force transducer installed with the active strut and an accelerometer mounted at a free end of the truss in the vertical direction were used to measure the response of the truss (see Fig. 2). Measured frequency response functions (FRF) at these sensor locations with respect to the input disturbance to the active strut are shown in Fig. 4. Note that multiple dominant frequencies appear in the FRF.

As described previously, the real-time system identification algorithm was developed on the basis of the assumption that a single mode is identified at a time. Because the disturbance is of random nature and the measured responses have multiple frequency contents in them, the signals need to be filtered to extract a single frequency. In this experiment, the signal corresponding to the second mode of the truss at about 17.5 Hz was extracted using a fourth-order Butterworth filter. The filter has a high-pass break frequency of 10 Hz and a low-pass break frequency of 25 Hz. Sampling frequency was set at 256 Hz. Filtered disturbance and response signals then were fed into the adaptive filter for filter coefficient update and modal parameter identification. This process is shown schematically in Fig. 5. The results of the filter coefficient updates and the corresponding modal parameters of the second mode of the undamaged truss are shown in Figs. 6 and 7, respectively. Initially, the filter coefficients were set to zero. Figures 6 and 7 indicate rapid convergence to the correct values as the coefficient updating process begins at about 5 s. The natural frequency converged to about 17.5 Hz and the damping ratio to about 0.002. These values match well with those obtained using an independent modal test. The amplitudes are different because two sensors located at different places were used.

**Structural Damage Detection Experiment**

The real-time modal parameter identification algorithm was employed to detect structural damage of the NRL truss. In this experimental study, each damage case was produced by loosening a nut at one end of a strut. The consequence of the loosened nut is the loss of stiffness of the corresponding strut. Table 1 summarizes the damage cases. The locations of damaged struts are shown in Fig. 2. Modal strain energy (MSE) information for the second mode[17] was used to select the struts with varying degrees of MSE distribution. The struts with higher MSE produce larger changes in modal parameters and, therefore, their damage is expected to be easier to detect.

Prior to the damage detection experiments, the filter coefficients had been converged to those corresponding to the undamaged case, as shown in Fig. 6. While the real-time identification algorithm was continuously running, a nut was loosened and the changes in the identified modal parameters were monitored for the total duration of 120 s. Figures 8–11 show the experimental data obtained during the process. They display time histories of identified modal parameters using either a force transducer or an accelerometer signal for the same damage case. As indicated, loosening of the nut was started at about 30 s and it took about 15–20 s to untie it completely. The transient period in each plot resulted directly from this loosening process. Changes in modal parameters are immediately noticeable during the transient period, and some of the changes were permanent. These apparent changes in modal parameters indicate that there are structural anomalies in the truss and the anomalies are immediately detected by the real-time identification algorithm. As is shown, damage at different strut locations exhibits different patterns of the modal parameter changes. Damping ratios increased immediately for all the damage cases, reflecting that the truss was being held by hands and wrenches during the process of loosening a strut. Table 2

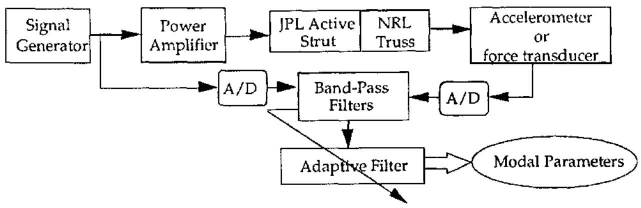


**Fig. 5 Modal parameter identification process.**

**Table 1 Summary of the damage cases**

| Damage case | Location of damage | Level of MSE for mode 2 |
|---|---|---|
| A | Diagonal in the center bay | High |
| B | Longeron near the center bay | Low |
| C | Batten in the ground bay | Medium |
| D | Longeron near the free end | Very low |

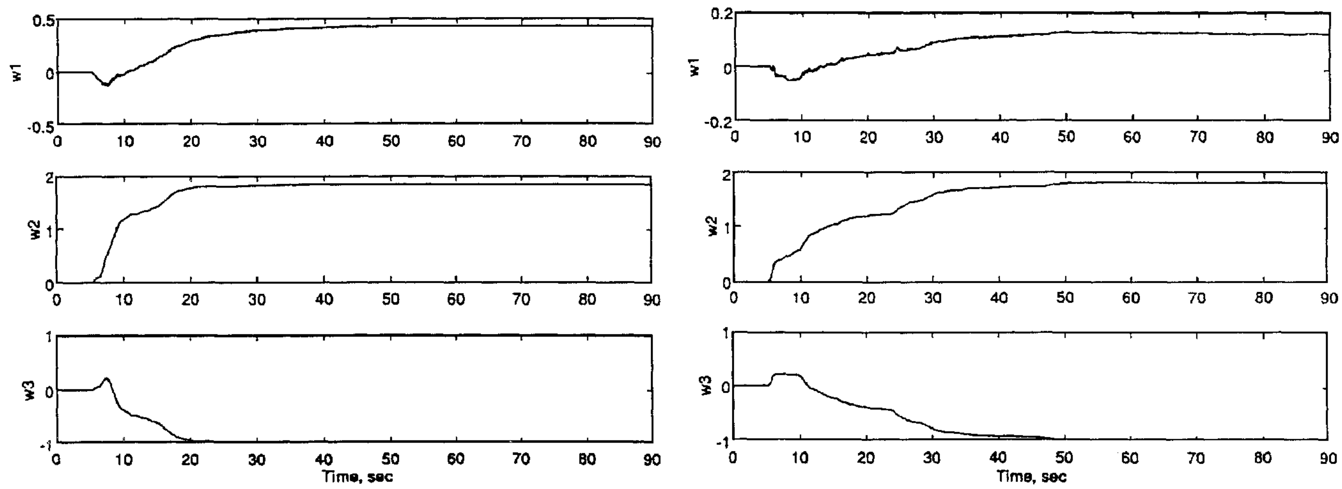


a) Using force transducer signal

b) Using accelerometer signal

**Fig. 6 Time history of updated filter coefficients for the undamaged truss.**

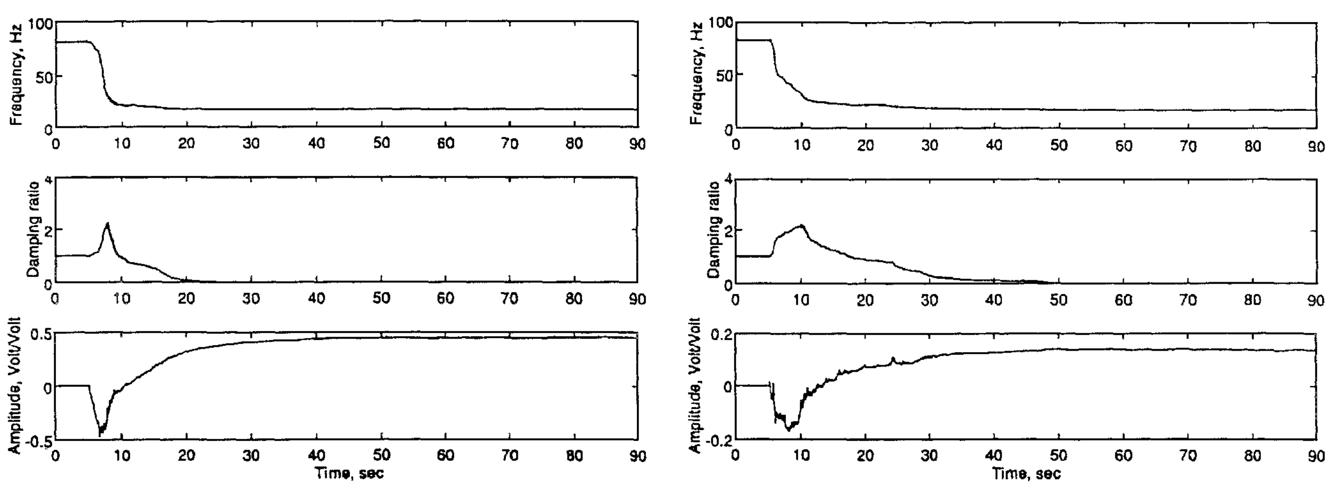


a) Using force transducer signal

b) Using accelerometer signal

**Fig. 7 Time history of updated modal parameters for the undamaged truss.**

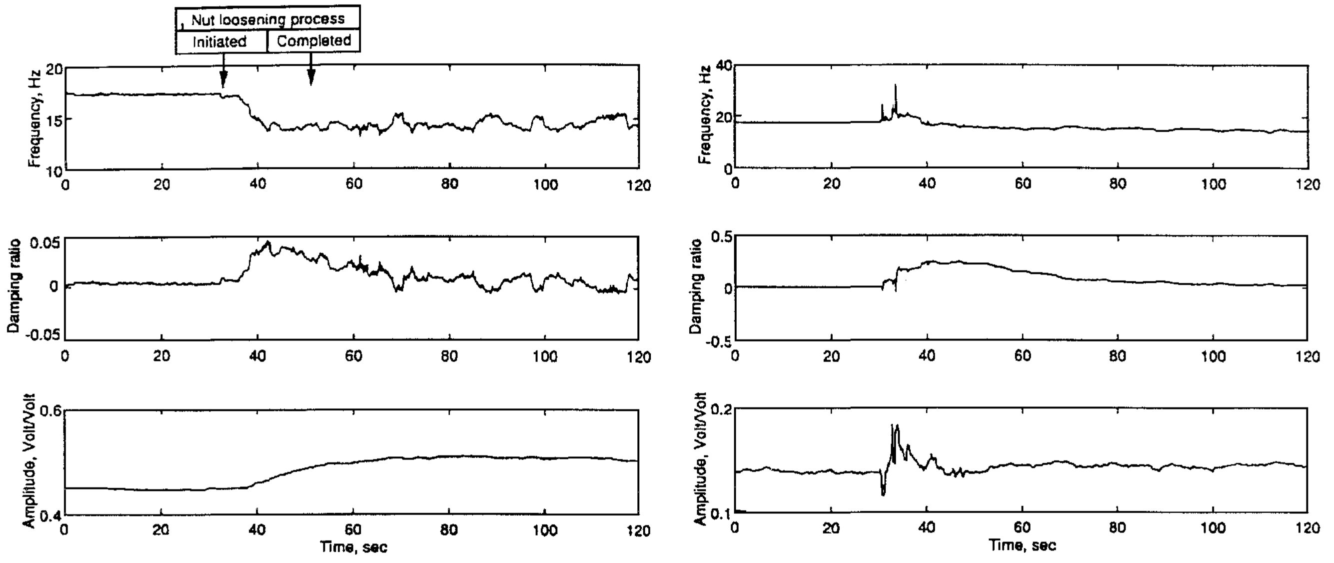


a) Using force transducer signal b) Using accelerometer signal

**Fig. 8 Results of real-time damage detection (case A).**

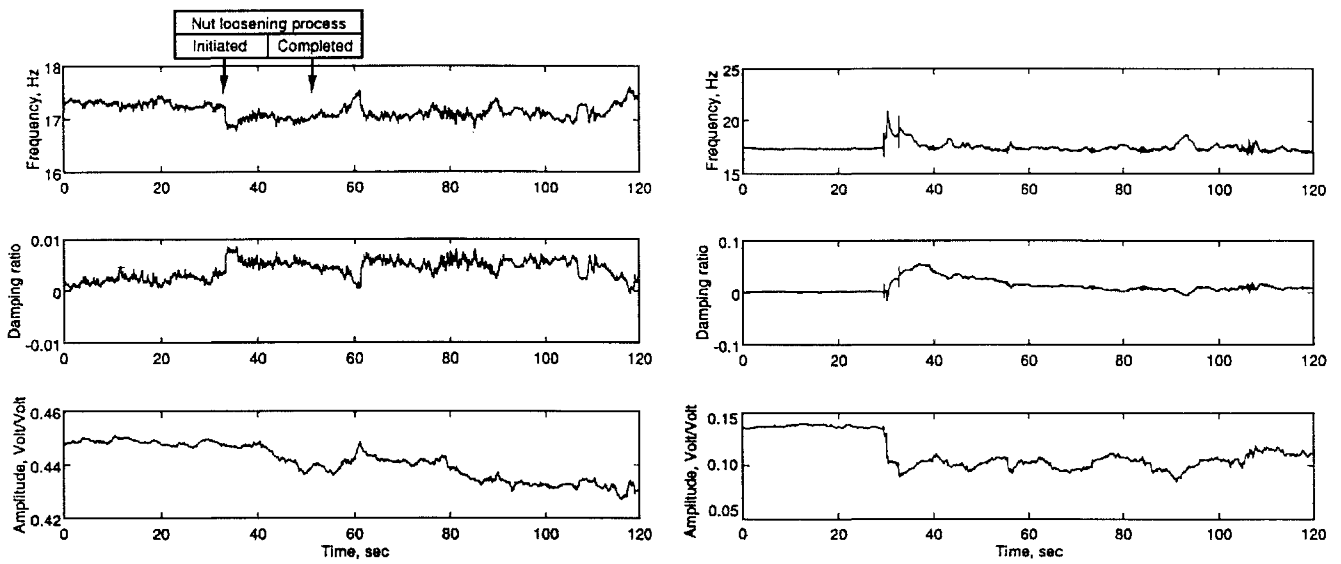


a) Using force transducer signal b) Using accelerometer signal

**Fig. 9 Results of real-time damage detection (case B).**

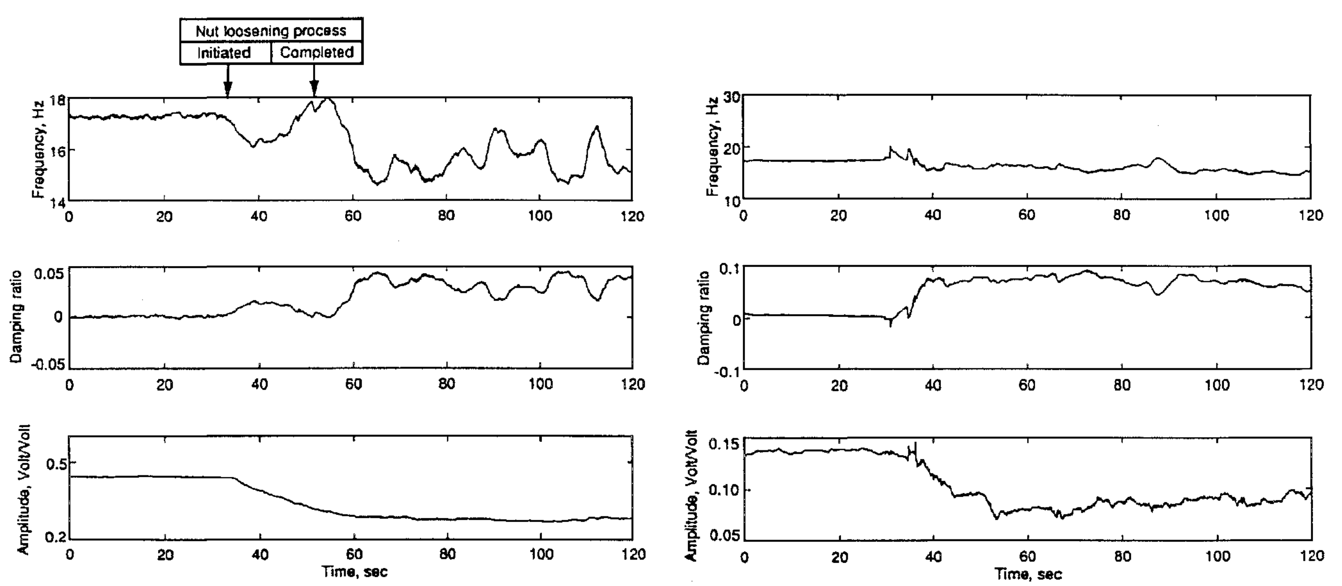


a) Using force transducer signal b) Using accelerometer signal

**Fig. 10 Results of real-time damage detection (case C).**

**Table 2 Changes in modal parameters before and after loosening a nut**

| | Before[a] | | | After[a] | | |
|---|---|---|---|---|---|---|
| Damage case | Frequency, Hz | Damping ratio | Amplitude | Frequency, Hz | Damping ratio | Amplitude |
| A | 17.30 | 0.0039 | 0.448 | 14.40 | 0.0072 | 0.508 |
| B | 17.29 | 0.0021 | 0.449 | 17.13 | 0.0047 | 0.436 |
| C | 17.28 | 0.0013 | 0.447 | 15.49 | 0.0325 | 0.279 |
| D | 17.26 | 0.0025 | 0.451 | 17.27 | 0.0019 | 0.449 |
| | Before[b] | | | After[b] | | |
| Damage case | Frequency, Hz | Damping ratio | Amplitude | Frequency, Hz | Damping ratio | Amplitude |
| A | 17.36 | 0.0037 | 0.139 | 15.03 | 0.0574 | 0.145 |
| B | 17.35 | 0.0022 | 0.137 | 17.41 | 0.0087 | 0.104 |
| C | 17.35 | 0.0054 | 0.137 | 15.59 | 0.0709 | 0.087 |
| D | 17.39 | 0.0023 | 0.136 | 17.36 | 0.0067 | 0.136 |

[a]Using the force transducer signal. [b]Using the accelerometer signal.

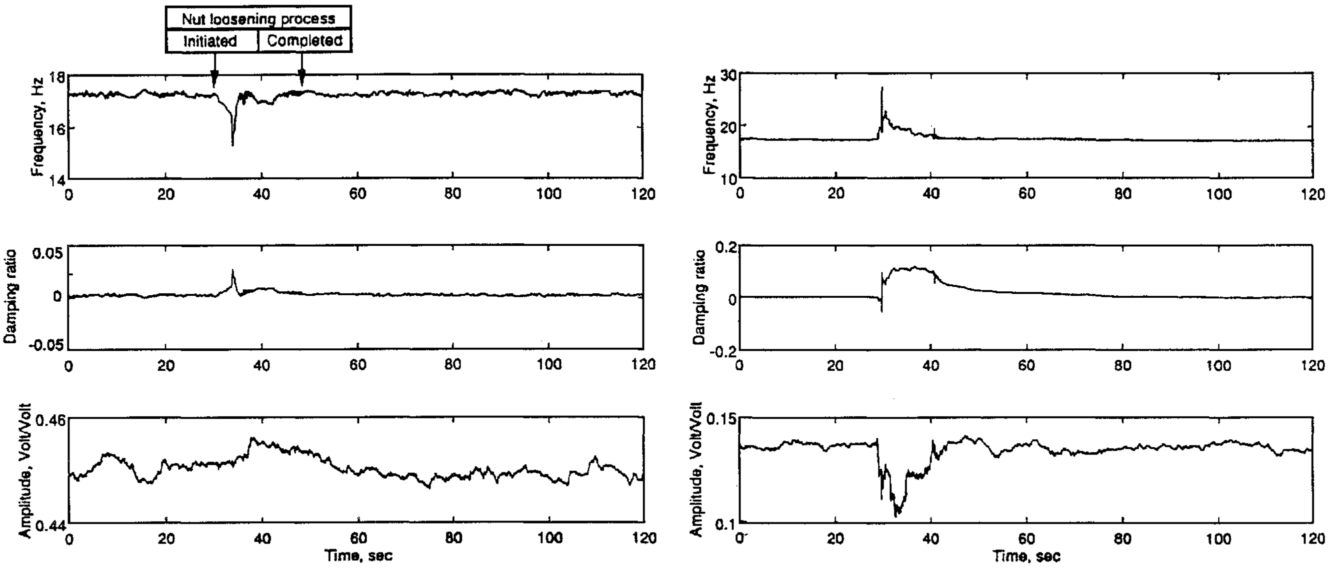


a) Using force transducer signal

b) Using accelerometer signal

**Fig. 11 Results of real-time damage detection (case D).**

summarizes the changes in modal parameters before and after the transient period, i.e., the process of loosening a nut, for each damage case. The identified natural frequencies and amplitudes before a nut is loosened are very consistent. Considering that the nut loosened to generate one damage case has to be tightened again before creating other damage case, the process of loosening and tightening a nut does not significantly affect the identified natural frequencies and amplitudes. Identified damping ratios are not as consistent, indicating that only significant changes in damping ratios shoud be alerted as anomalies.

For damage cases A, B, and C, changes in at least one modal parameter became permanent after the transient period, as indicated in Table 2 and Figs. 8–11. For damage case A, for instance, the natural frequency obtained using the force transducer signal dropped from 17.3 to 14.4 Hz indicating anomaly in the truss, i.e., structural damage. Apparent drop in amplitude measured using the accelerometer signal for damage cases B and C and significant damping increase for damage case C indicate permanent anomalies in the truss. The results also depend on the sensor signal employed in the identification process. The truss-tip-mounted accelerometer produces clearer change in amplitude for case B, whereas the force transducer shows easily noticeable change in amplitude for case A. For case D, although the transient period is pronounced, the changes before and after the transient period are difficult to notice, indicating that the second mode is not appropriate to detect the damage in the strut near the tip of the truss. Considering that such strut carries very low strain energy in the lower frequency modes, higher modes will be required to detect the damage successfully.

## Concluding Remarks

It was clearly demonstrated experimentally that the real-time modal parameter identification algorithm is capable of detecting anomalies in the structure such as loss of stiffness. The real-time identification algorithm reports changes in modal parameters immediately as they happen. This capability will give an operator early warning so that appropriate action may be taken before a catastrophic failure occurs. Although the study shows that the algorithm is capable of detecting damage, pinpointing the location of the damaged member and estimating the extent of damage are not addressed. To address these issues, the modal parameter identification should be conducted for several important modes in the truss and more sensors should be placed at strategic locations. A database containing patterns of modal parameter changes attributable to various damage scenarios and a method of classifying measured data also will be needed to identify damage location and magnitude. Further investigations are under way to address these issues.

## Acknowledgment

The first author was supported by a U.S. Navy/American Society for Engineering Education Summer Faculty Research Fellowship at the NRL in Washington, D.C.

## References

[1]Hajela, P., and Soeiro, F., "Recent Developments in Damage Detection Based on System Identification Methods," *Structural Optimization*, Vol. 2, No. 1, 1990, pp. 1–10.

[2]Simmermacher, T., Zimmerman, D. C., Mayes, R. L., Reese, G. M., and James, G. H., "The Effects of Finite Element Grid Density on Model Correlation and Damage Detection of a Bridge," AIAA Paper 95-1075, April 1995.

[3]Lima Torres, A., and Partes de Lima, E., "Fatigue Damage Prediction in Steel Structures by Dynamic and Pseudo Static Analysis," *Proceedings of the 5th International Symposium on Offshore Engineering*, Pentech, London, 1985, pp. 33–44.

[4]Zimmerman, D. C., and Kaouk, M., "Structural Damage Assessment Using a Generalized Minimum Rank Perturbation Theory," *AIAA Journal*, Vol. 32, No. 4, 1994, pp. 836–842.

[5]Lim, T. W., and Kashangaki, T. A.-L., "Structural Damage Detection of Space Truss Structures Using Best Achievable Eigenvectors," *AIAA Journal*, Vol. 32, No. 5, 1994, pp. 1049–1057.

[6]Kim, H. M., and Bartkowicz, T. J., "A Two-Step Structural Damage Detection Approach with Limited Instrumentation," *Proceedings of the AIAA Dynamics Specialists Conference*, AIAA, Washington, DC, 1994, pp. 318–324.

[7]Li, C., and Smith, S. W., "Hybrid Approach for Damage Detection in Flexible Structures," *Journal of Guidance, Control, and Dynamics*, Vol. 18, No. 3, 1995, pp. 419–425.

[8]Tsou, P., and Shen, M.-H. H., "Structural Damage Detection and Identification Using Neural Networks," *AIAA Journal*, Vol. 32, No. 1, 1994, pp. 176–183.

[9]Povich, C. R., and Lim, T. W., "An Artificial Neural Network Approach to Structural Damage Detection Using Frequency Response Functions," *Proceedings of the AIAA/ASME Adaptive Structures Forum*, AIAA, Washington, DC, 1994, pp. 151–159.

[10]Kirby, G. C., Bosse, A. B., Fisher, S., and Lindner, D. K., "Damage Assessment of a Precision Truss Using Identified Modal Parameters," 10th VPI&SU Symposium on Structural Dynamics and Control, Blacksburg, VA, May 1995.

[11]Lim, T. W., Bosse, A., and Fisher, S., "Adaptive Filters for Real-Time System Identification and Control," AIAA Paper 96-1204, April 1996.

[12]Lim, T. W., Cabell, R. H., and Silcox, R. J., "On-Line Identification of Modal Parameters Using Artificial Neural Networks," *Journal of Vibration and Acoustics* (to be published).

[13]Ogata, K., *Discrete-Time Control Systems*, 2nd ed., Prentice–Hall, Englewood Cliffs, NJ, 1995.

[14]Widrow, B., and Stearns, S. D., *Adaptive Signal Processing*, Prentice–Hall, Englewood Cliffs, NJ, 1985.

[15]Macchi, O., *Adaptive Processing—The Least Mean Square Approach with Application in Transmission*, Wiley, Chichester, England, UK, 1995.

[16]Fanson, J. L., Blackwood, G. H., and Chu, C.-C., "Active-Member Control of Precision Structures," *Proceedings of the AIAA/ASME/ASCE/AHS/ASC Structures, Structural Dynamics, and Materials Conference*, AIAA, Washington, DC, 1989, pp. 1480–1494.

[17]Lim, T. W., and Waner, R. C., "System Identification, Control, and Health Monitoring of the NRL Space Truss Structure," Flight Research Lab., Univ. of Kansas Center for Research, Inc., Final Rept. KU-FRL-1159-1, Lawrence, KS, Aug. 1995.